Published OnlineFirst September 8, 2009; DOI: 10.1158/0008-5472.CAN-09-1304

Anticancer Activity of CX-3543: A Direct Inhibitor of rRNA Biogenesis

Denis Drygin,[1] Adam Siddiqui-Jain,[1] Sean O'Brien,[1] Michael Schwaebe,[1] Amy Lin,[1] Josh Bliesath,[1] Caroline B. Ho,[1] Chris Proffitt,[1] Katy Trent,[1] Jeffrey P. Whitten,[1] John K. C. Lim,[1] Daniel Von Hoff,[2] Kenna Anderes,[1] and William G. Rice[1]

[1]Cylene Pharmaceuticals, Inc., San Diego, California and [2]Translational Genomics Research Institute, Phoenix, Arizona

Abstract

Hallmark deregulated signaling in cancer cells drives excessive ribosome biogenesis within the nucleolus, which elicits unbridled cell growth and proliferation. The rate-limiting step of ribosome biogenesis is synthesis of rRNA (building blocks of ribosomes) by RNA Polymerase I (Pol I). Numerous kinase pathways and products of proto-oncogenes can up-regulate Pol I, whereas tumor suppressor proteins can inhibit rRNA synthesis. In tumorigenesis, activating mutations in certain cancer-associated kinases and loss-of-function mutations in tumor suppressors lead to deregulated signaling that stimulates Pol I transcription with resultant increases in ribosome biogenesis, protein synthesis, cell growth, and proliferation. Certain anticancer therapeutics, such as cisplatin and 5-fluorouracil, reportedly exert, at least partially, their activity through disruption of ribosome biogenesis, yet many prime targets for anticancer drugs within the ribosome synthetic machinery of the nucleolus remain largely unexploited. Herein, we describe CX-3543, a small molecule nucleolus-targeting agent that selectively disrupts nucleolin/rDNA G-quadruplex complexes in the nucleolus, thereby inhibiting Pol I transcription and inducing apoptosis in cancer cells. CX-3543 is the first G-quadruplex interactive agent to enter human clinical trials, and it is currently under evaluation against carcinoid/neuroendocrine tumors in a phase II clinical trial. [Cancer Res 2009;69(19):7653–61]

Introduction

The availability of ribosomes is a key regulator of cell growth and proliferation (reviewed in ref. 1). Ribosome biogenesis occurs in the nucleolus and is carefully controlled by multiple cell signaling pathways that converge on the RNA Polymerase I complex (Pol I). Pol I is directly responsible for transcription of *rRNA* genes to generate pre-rRNAs that are processed to mature rRNA molecules, the key building blocks of ribosomes (reviewed in ref. 2). Because rRNA synthesis is the rate-limiting step of ribosome biogenesis (3), Pol I is highly regulated (reviewed in ref. 4), and many of its regulators play critical roles in cancer (reviewed in refs. 5–8). Deregulated signaling by proto-oncogenes and tumor suppressors activates Pol I to accelerate ribosome biogenesis and support rapid cell proliferation of cancer cells (9–12). The link between nucleolar hypertrophy and tumorigenesis has been recognized for more than a century (13). More recent data show that a marked increase in rRNA synthesis is a general phenomenon in cancer, that the rate of cancer cell proliferation in tumors is directly proportional to nucleolar size and Pol I activity, and that overexpression of pre-rRNA correlates with an adverse prognosis in cancer (14, 15). Although several approved anticancer therapeutics have been shown to inhibit rRNA biogenesis (16, 17), there are currently no approved agents that specifically target Pol I transcription. Low concentrations of actinomycin D have been shown to preferentially inhibit rRNA synthesis over mRNA synthesis. However, its selectivity is questionable as it affects other cellular processes, such as the maturation of mRNA, at the same concentrations (18). Thus, structures and processes of the rRNA synthesis pathway represent important, but largely unexploited, targets for anticancer drugs.

Human ribosomal DNA (rDNA) is GC rich. It contains >400 copies of the *rRNA* genes, organized in tandem arrays on five different human chromosomes (reviewed in ref. 4). Transcription of G-rich templates, such as rDNA, is accompanied by the formation of G-quadruplex DNA structures in nontemplate strands (19). These structures can prevent renaturation of the template DNA, thereby promoting the dense spacing of Pol I molecules on *rRNA* genes, which is characteristic of rapidly transcribing rDNA (it can be as high as one Pol I per 41 nucleotides; ref. 20). Indeed, treatment of yeast with a G-quadruplex–targeting porphyrin selectively down-regulates rRNA expression, indicating the formation of G-quadruplexes in rDNA *in vivo* as well as their potential role in rRNA biogenesis (21). Nucleolin, an abundant nucleolar protein (22), is associated with rDNA *in vivo* and is absolutely required for rRNA synthesis, as its knockdown was shown to specifically inhibit Pol I–driven transcription (23, 24). Nucleolin possesses nanomolar affinities for such G-quadruplex structures (25) and thus may bind to and further stabilize them to increase the rate of Pol I transcription. Thus, targeting nucleolin/rDNA G-quadruplex complexes to inhibit aberrant Pol I transcription in cancer cells represents a novel, nucleolus targeting approach to selectively disrupt proliferation of cancer cells.

Extensive research efforts identified CX-3543 (also known as quarfloxin; Fig. 1*A*), a small molecule fluoroquinolone derivative that targets and disrupts nucleolin/rDNA G-quadruplex complexes. Fluoroquinolone antibiotics bind duplex DNA and inhibit bacterial gyrase, inducing selective cytotoxicity in bacterial cells (26). Similarly, CX-3543 binds to G-quadruplex DNA and was shown to selectively disrupt interaction of rDNA G-quadruplexes with the nucleolin protein thereby inhibiting Pol I transcription and inducing apoptotic death in cancer cells.

Materials and Methods

CX-3543. Stock solution [10 mg/mL (16.5 mmol/L)] of CX-3543 (99.2–99.5% pure) in 10% polyethylene glycol 300, 2% mannitol, and

Note: Supplementary data for this article are available at Cancer Research Online (http://cancerres.aacrjournals.org/).

Requests for reprints: William G. Rice, Cylene Pharmaceuticals, 5820 Nancy Ridge Drive, Ste 200, San Diego, CA 92121. Phone: 858-875-5100; Fax: 858-875-5101; E-mail: wrice@cylenepharma.com.

doi:10.1158/0008-5472.CAN-09-1304

Published OnlineFirst September 8, 2009; DOI: 10.1158/0008-5472.CAN-09-1304

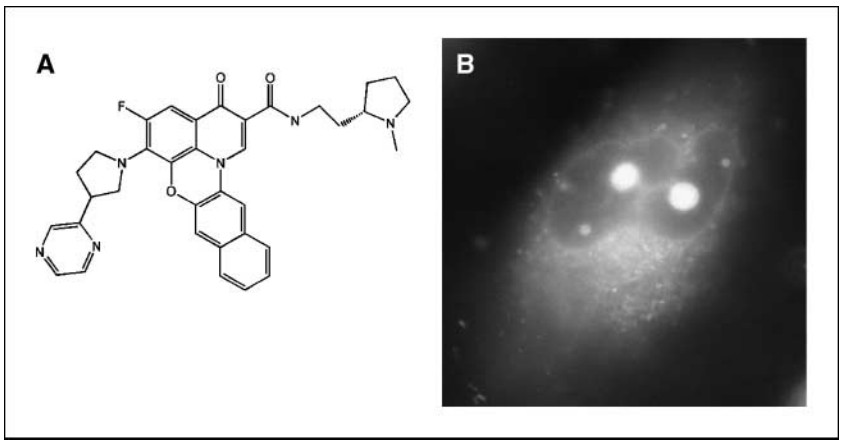

Figure 1. CX-3543 concentrates in the nucleoli of cancer cells. *A,* structure of CX-3543. *B,* A549 lung carcinoma cells were treated with 5 μmol/L CX-3543 for 1 h, washed, and visualized using Olympus IX2 series microscope with open channel UV filter and ×60 objective.

25 mmol/L phosphate buffer (pH 6) was stored at room temperature in the dark. The drug was diluted directly in growth media before treatment.

Cell lines. Lung carcinoma A549 cells, colorectal adenocarcinoma HCT-116 cells, breast adenocarcinoma MDA-MB-231 cells, breast adenocarcinoma MCF7 cells, pancreatic carcinoma MIA PaCa-2 cells, and acute promyelocytic leukemia HL-60 were purchased from American Tissue Culture Collection.

Circular dichroism analysis of rDNA PQSs. Oligonucleotides corresponding to PQSs from the nontemplate strand of rDNA were purchased from Invitrogen, denatured at 100°C for 5 min, and gradually brought to ambient temperature in the presence of potassium ions. The circular dichroism spectra of G-quadruplexes were measured with Jasco J-810 Spectropolarimeter. The G-quadruplexes with a spectrum containing a positive maximum at 260 nm were deemed as predominantly parallel, whereas G-quadruplexes with a spectrum containing a positive maximum at 295 nm were deemed as predominantly antiparallel. Those that exhibited both features were assigned a mixed conformation.

Interaction of nucleolin protein with rDNA G-quadruplexes and competition by CX-3543. rDNA G-quadruplexes were labeled with ^{32}P at the 5′-end using T4 polynucleotide kinase (New England Biolabs). Affinity of various G-quadruplexes for recombinant human nucleolin (a kind gift of Dr. Maizels, University of Washington, Seattle, WA) was measured by filter-binding assay. In summary, 0.1 nmol/L of ^{32}P-labled rDNA quadruplex was incubated for 30 min at ambient temperature with 0.3 to 30 nmol/L of nucleolin in a binding buffer containing 12.5 mmol/L Tris (pH 7.6), 60 mmol/L KCl, 1 mmol/L $MgCl_2$, 0.1 mmol/L EDTA, 5% glycerol, and 100 μg/mL bovine serum albumin (BSA). The resulting complexes were filtered through mixed cellulose ester membranes (Millipore). The membranes were washed thrice, dried, and counted in a Microbeta Trilux 2 detection system (Perkin-Elmer). Dissociation constants (K_d) were calculated using GraphPad Prism software (GraphPad Software). For the competition studies, a mix of 5 nmol/L of ^{32}P-labeled rDNA G-quadruplex and 10 nmol/L nucleolin were incubated in binding buffer 30 min at ambient temperature with 0.3 to 30 μmol/L CX-3543. The resulting complexes were resolved using Novex Tris-borate EDTA DNA retardation PAGE (Invitrogen). The gels were dried and exposed to X-ray film (Kodak). Inhibition constants were calculated using the Cheng-Prusoff equation: $K_i = IC_{50}/(1+N/K_d)$, where K_i is inhibition constant, IC_{50} is a median inhibition concentration, N is the concentration of nucleolin, and K_d is a dissociation constant for the nucleolin/rDNA G-quadruplex complex.

Table 1. PQS in rDNA

Name	Sequence (a)	CD (b)	K_d (nmol/L; c)	K_i (nmol/L; d)
1196NT	5′-GGGTGGACGGGGGGGCCTGGTGGGG-3′	M	1.1 ± 0.4	252
2957NT	5′-GGGTCGGGGGGTGGGGCCCGGGCCGGGG-3′	M	1.5 ± 0.2	135
5701NT	5′-AGGGAGGGAGACGGGGGGG-3′	M	1.0 ± 0.2	277
6183NT	5′-GGGTCGGGGGCGGTGGTGGGCCCGCGGGGG-3′	M	1.9 ± 0.6	317
6374NT	5′-GGGGGCGGGAACCCCCGGGCGCCTGTGGG-3′	M	1.4 ± 0.4	320
6534NT	5′-GGGCGGGGGGGGCGGGGGG-3′	P	0.6 ± 0.2	98
6960NT	5′-GGGTGGCGGGGGGGAGAGGGGGG-3′	P	0.2 ± 0.1	18
7253NT	5′-GGGTCCGGAAGGGGAAGGGTGCCGGCGGGG AGAGAGGGTCGGGGG-3′	M	0.4 ± 0.2	165
8511NT	5′-GGGGGCGGGCTCCGGCGGGTGCGGGGGTGG GCGGGCGGGGCCGGGGGTGGGGTCGGCGGGGG-3′	M	0.6 ± 0.1	245
8749NT	5′-GGGAGGGCGCGCGGGTCGGGG-3′	A	ND	NA
10816NT	5′-GGGCTGGGTCGGTCGGGCTGGGG-3′	A	ND	NA
11028NT	5′-GGGGCGCGGCGGGGGGAGAAGGGTCGGGGCGGCAGGGG-3′	M	0.4 ± 0.3	ND
13079NT	5′-GGGGTGGGGGGGAGGG-3′	P	0.5 ± 0.3	83
13173NT	5′-GGGCCGGGACGGGGTCCGGGG-3′	M	ND	NA

NOTE: G-quadruplex conformations of oligonucleotides corresponding to PQS in rDNA (a) were determined by circular dichroism (*CD*; b); Nucleolin/G-quadruplex binding affinities (K_d) were assayed by filter binding (Mean ± SEM; c); and the potential of CX-3543 to disrupt nucleolin/G-quadruplex complexes (K_i) by gel mobility shift (d).
Abbreviations: P, parallel; A, antiparallel; M, mixed; ND, not detected; NA, not applicable.

Published OnlineFirst September 8, 2009; DOI: 10.1158/0008-5472.CAN-09-1304

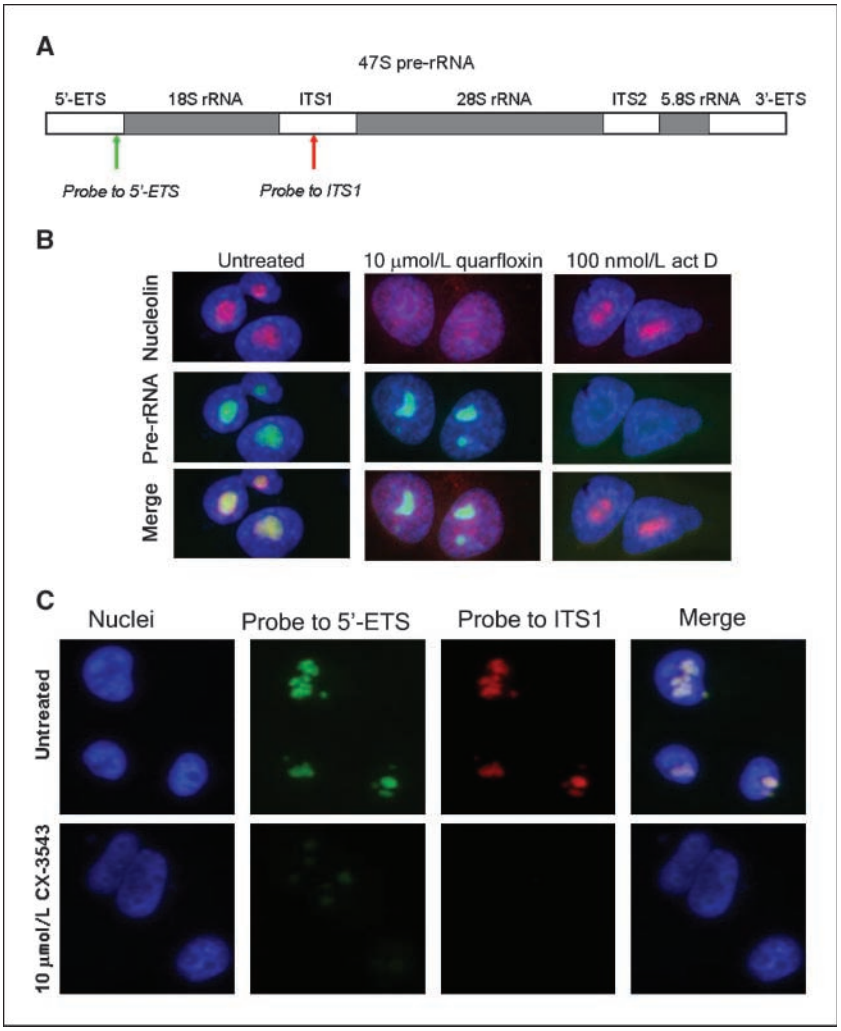

Figure 2. CX-3543 causes redistribution of nucleolin protein from nucleoli into the nucleoplasm before inhibition of rRNA synthesis. *A,* 47S pre-rRNA. *B,* A549 cells, untreated or treated for 2 h with 10 μmol/L CX-3543 or 100 nmol/L actinomycin D (*act D*), were washed, fixed, and analyzed by a combination of immunocytochemistry and FISH using antinucleolin mouse monoclonal antibody coupled with Cy3-labeled secondary antibody (*red*) and Alexa-488–labeled probe that hybridizes to 5′-external transcribed spacer (*5′-ETS*) of short-lived pre-rRNA (*green*). Cellular nuclei were stained with Hoescht 33342 (*blue*) and cells were visualized with Zeiss Axiovert 200 microscope using ×40 objective. *C,* A549 cells, untreated or treated for 4 h with 10 μmol/L CX-3543, were washed, fixed, and analyzed by FISH using Alexa-488 labeled probe that hybridizes to 5′-external transcribed spacer (*green*) and Cy3-labeled probe that hybridizes to internal transcribed spacer 1 (*ITS1*; *red*) regions of short-lived pre-rRNA. Cellular nuclei were stained with Hoescht 33342 (*blue*) and cells were visualized with Zeiss Axiovert 200 microscope using ×40 objective.

Immunocytochemistry. A549 cells were plated in F12 media supplemented with 10% fetal bovine serum on poly-L-lysine coated slides (EMS). After overnight incubation, cells were treated with indicated doses of drugs for specified periods of time. After treatment, cells were washed twice with PBS, fixed for 10 min in 4% paraformaldehyde/PBS, washed twice again with PBS and permeabilized for 10 min in 100% ethanol, washed thrice with PBS, blocked for 30 min with 5% donkey serum (Invitrogen) in PBS with 0.05% Tween 20, and incubated 1 h with either 1:500 dilution of mouse monoclonal antinucleolin antibody (Stressgen), 1:100 dilution of rabbit polyclonal anti–cleaved caspase-3 or rabbit polyclonal anti-fibrillarin antibody (Cell Signaling Technology) in 5% donkey serum (Invitrogen). Then cells washed thrice for 5 min with PBS; incubated for 30 min with 1:100 dilution of Cy3-linked goat anti-mouse secondary antibody, FITC-, or Cy3-linked goat anti-rabbit secondary antibody (Invitrogen); washed thrice for 15 min with PBS; and visualized on a Zeiss Axiovert 200 fluorescence microscope (Zeiss).

Fluorescent *in situ* hybridization. A549 cells were incubated overnight on poly-L-lysine–coated slides then treated with indicated doses of CX-3543 for specified periods of time. Cells then were washed twice with PBS, fixed for 10 min in 4% paraformaldehyde/PBS (pH 8.0) at room temperature, washed twice again with PBS, and permeabilized for 10 min in 100% ethanol. Cells then were washed twice with 10% formamide in 2 × SSC buffer and hybridized for 3 h at 37°C with 2.5 ng/μL of fluorescently labeled probe that hybridizes to the 5′-external transcribed spacer (5′-/Alexa488(or Cy3)/-TGAGAGCACGACGTCACCACATCGATCGAAGAGC-3′) or internal transcribed spacer 1 (5′-Alexa488-TGAGAGCACGACGTCACCACATCGATC-GAAGAGC-3′) of pre-rRNA in a buffer containing 10% formamide, 0.5 μg/mL yeast tRNA, 10% dextran, 50 μg/mL BSA, and 10 mmol/L ribonucleoside vanadyl complexes in 2× SSC. The slides were washed twice for 5 min with 10% formamide in 2× SSC buffer and once with PBS followed by the incubation for 5 min with 1 μmol/L solution of Hoescht 33342 in PBS. Then the cells were washed twice with PBS and visualized on Zeiss Axiovert 200 fluorescence microscope (Zeiss,).

Chromatin immunoprecipitation. A549 cells were seeded at 1.5×10^6 cells per 150-mm plate 1 d before 2-h treatment with 10 μmol/L with CX-3543. The assays were then carried out as described previously (27) with the following modifications. The nuclear lysate was sonicated to generate 200 to 500 bp chromatin fragments. For each immunoprecipitation, the precleared lysate (equivalent to $\sim 3 \times 10^6$ cells) was incubated with 4 μL of rabbit nonimmune serum or rabbit serum against UBF or TATA binding protein or 1.5 μg of antinucleolin rabbit polyclonal antibody (Novus Biologicals) overnight at 4°C. PCR was performed in 50 μL of reaction mixture containing 4 μL of DNA, 25 μL of 2 × SYBR Green PCR Master Mix (Applied Biosystems), and 250 nmol/L primers. Accumulation of fluorescent product was monitored by real-time PCR using 7900HT Real-time PCR System (Applied Biosystems). The sequences of primers used in the PCR are as follows: −48, 5′-CCCGGGGGAGGTATATCTTT-3′ and 5′-CCAACCTCTCC-GACGACA-3′; +2907, 5′-GACGTGTGGCGTGGGTCGAC-3′and 5′-GACGG-GAGGCAGCGACCGG-3′; +5645, 5′-GTTCGCTCGCTCGTTCGTTC-3′ and 5′-CAACGACACGCCCTTCTTTC-3′; and +12855, 5-ACCTGGCGCTAAAC-CATTCGT -3 and 5-GGACAAACCCTTGTGTCGAGG-3. A series of dilutions of input DNA were run alongside the chromatin immunoprecipitation samples to establish the standard curve for each pair of primers. The background from the control reaction (nonimmune serum) was <0.0001% of input chromatin and was subtracted from the data of the sample reactions.

Published OnlineFirst September 8, 2009; DOI: 10.1158/0008-5472.CAN-09-1304

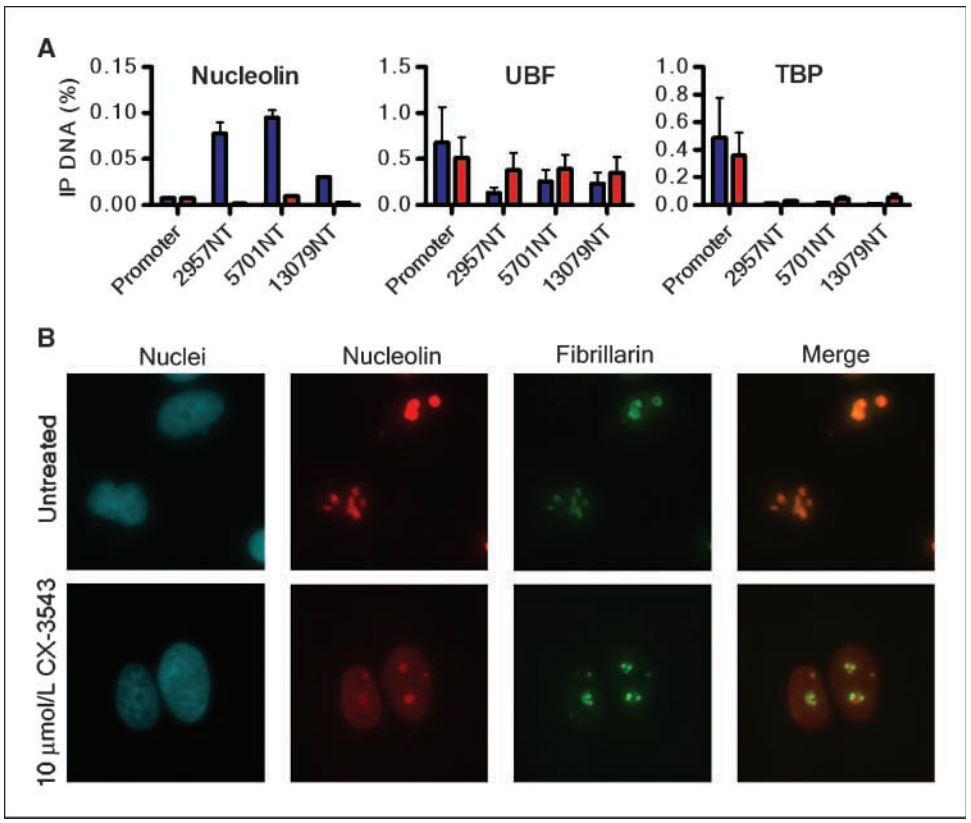

Figure 3. CX-3543 selectively competes nucleolin from PQS on rDNA. *A,* chromatin immunoprecipitation analysis of nucleolin, UBF, and TATA binding protein (*TBP*) associations with indicated sites in the rDNA of A549 cells, untreated (*blue bar*) or treated with 10 μmol/L CX-3543 (*red bar*) for 2 h. *B,* A549 cells, untreated or treated for 2 h with 10 μmol/L CX-3543, were fixed and analyzed by immunocytochemistry using mouse monoclonal antinucleolin antibody coupled with Cy3-labeled secondary antibody (*red*) and rabbit polyclonal antifibrillarin antibody coupled with FITC-labeled secondary antibody (*green*). Cellular nuclei were stained with 4′,6-diamidino-2-phenylindole (*cyan*) and cells were visualized with Zeiss Axiovert 200 microscope using ×40 objective.

Nuclear run-on. Isolated nuclei (8×10^5) from HCT-116 cells using Nuclei Isolation kit (Sigma-Aldrich) were incubated for 30 min at ambient temperature in buffer containing 120 mmol/L KCl; 2.5 mmol/L $MgCl_2$; 500 μmol/L each GTP, ATP, UTP, and CTP; 1 μCi [α-^{32}P]GTP (Perkin-Elmer); and 10 μg/mL α-amanitin (Sigma-Aldrich) with 0.3 to 30 μmol/L of CX-3543. After incubation, total RNA was isolated using RNeasy kit (QIAGEN), its concentration was determined using Ribogreen reagent (Invitrogen), and specific activity was measured with Microbeta Trilux 2 detection system (Perkin-Elmer).

qRT-PCR. A549 cells were plated on 96-well plates and treated the next day with 0.08 to 25 μmol/L of CX-3543 for 2 h. The RNA was isolated from cells using RNeasy kit (QIAGEN) and relative levels of pre-rRNA and bcl-2, c-myb, c-*myc*, and k-ras mRNA were measured using Applied Biosystems' proprietary primers-probe set for bcl-2, c-myb, c-*myc*, and k-ras mRNA and custom primers-probe set (forward primer, CCGCGCTCTACCTTACCTACCT; reverse primer, GCATGGCTTAATCTTTGAGACAAG; probe, TTGATCCTGCCAGTAGC) for pre-rRNA. Analysis was run on 7900HT Real-time PCR System (Applied Biosystems).

***In vivo* efficacy in mouse xenografts.** Five- to 6-wk-old female severe combined immunodeficient mice (IcrTac:ICR-*Prkdc*^{scid}) mice (Taconic Farms) or athymic (NCr *nu/nu* fisol) mice of BALB/c origin (Simons Laboratories) were ear punched for identification and housed four per cage in ventilated microisolator cages maintained under pathogen-free conditions. Animals were provided *ad libitum* access to irradiated food and autoclaved water. Animal experiments were performed in accordance with approved standard operating protocols of Cylene Pharmaceuticals that were approved by the Institutional Animal Care and Use Committee. MDA-MB-231 and MIA PaCa-2 cells were obtained from American Type Culture Collection and cultured according to recommended specifications. Mice were inoculated with 1×10^7 cells per mouse in a 50% growth media/50% Matrigel (BD Bioscences) mixture directly into the inguinal mammary fat pad (MDA-MB-231) or 5×10^6 in 100 μL of cell suspension subcutaneouly in the right flank (MIA PaCa-2). Tumor measurements were performed by caliper, and tumor volume was calculated using the formula $(l \times w^2)/2$, where w is width and l is length in mm of the tumor. Established tumors (>125 mm^3) were randomized into vehicle (5% dextrose in water) or CX-3543 treatment groups. For the MDA-MB-231 model, CX-3543 (6.25 or 12.5 mg/kg) was administered via i.v. injection according to a 5-2-5 regimen (5-d treatment with 2-d rest) for 37 d. In MIA PaCa-2 xenografts, CX-3543 (5 mg/kg) was administered i.v. once daily for 13 d followed by 7 d of rest, followed by an additional 5 d of treatment.

Results

CX-3543 disrupts nucleolin/G-quadruplex complexes on rDNA. Several reports have quantified the prevalence of putative G-quadruplex forming sequences (PQS) in nonrepetitive regions of the human genome (28–30). To evaluate this potential for PQS in the repetitive and G-rich rDNA, we designed a search algorithm (quad_find; see Supplementary Materials and Methods) that identified 14 PQS in the nontemplate strand of each human *rRNA* gene (Table 1). Circular dichroism analysis of oligonucleotides corresponding to these PQS confirmed that all could form G-quadruplex structures of the parallel, antiparallel, or mixed conformations (Supplementary Fig. S1*A*; Table 1). Of the 14 PQS in the nontemplate strand of rDNA, all but three formed complexes with nucleolin characterized by K_d of <2 nmol/L, with six having K_d of <1 nmol/L. Interestingly, nucleolin exhibited selectivity for quadruplexes with parallel or mixed conformations. CX-3543 disrupted all but one of the identified nucleolin/G-quadruplex complexes with submicromolar inhibition constants (K_i), as determined by electrophoretic mobility shift assays (Supplementary Fig. S1*B* and *C*; Table 1), but did not interfere with the interaction between nucleolin and its other known ligand, hairpin RNA (Supplementary Fig. S1*C*; ref. 31).

CX-3543 accumulates in nucleoli of cancer cells, and causes redistribution of nucleolin followed by inhibition of rRNA synthesis. CX-3543 is a fluorescent molecule with excitation

Published OnlineFirst September 8, 2009; DOI: 10.1158/0008-5472.CAN-09-1304

maximum at 350 nm and emission maximum at 550 nm. Using fluorescence microscopy, we observed that CX-3543 rapidly accumulates in the nucleoli of A549 lung carcinoma cells (see Supplementary Materials and Methods; Fig. 1*B*). To determine the effects of CX-3543 on intracellular localization of nucleolin and rRNA synthesis, we used a combination of immunocytochemistry and fluorescent *in situ* hybridization (FISH) analyses. The 28S, 18S, and 5.8S rRNAs are initially transcribed as one short-lived 47S pre-rRNA precursor (Fig. 2*A*). Because the half-life of mature rRNAs is very long, we designed probes that hybridize to external or internal transcribed spacers within pre-rRNA to measure the effect of drugs on Pol I transcription. Two-hour treatment of the cells with CX-3543 was accompanied by a dramatic relocalization of nucleolin from nucleoli to the nucleoplasm of treated cells (Fig. 2*B, left* and *center top*). Certain drugs, such as actinomycin D, can intercalate into GC-rich regions of rDNA and also trigger the relocalization of nucleolin by inhibiting rRNA synthesis (32); in that case, a loss of staining for pre-rRNA in the nucleolus of A549 cells sequentially precedes the relocalization of nucleolin from the nucleolus to the nucleoplasm (e.g., Fig. 2*B, right*). In contrast, CX-3543–treated A549 cells showed nucleolin redistribution before a loss of pre-rRNA (e.g., Fig. 2*B, center*). Although inhibition of rRNA synthesis by CX-3543 was evident after 2-hour treatment (data not shown), 4-hour treatment resulted in complete depletion of pre-rRNA species from A549 cells (Fig. 2*C*). Certain types of cellular stress, such as treatment with camptothecin, can also affect the localization of nucleolin in p53-expressing cells (33). CX-3543 was able to redistribute nucleolin in the p53-null human osteosarcoma cell line Saos-2 (Supplementary Fig. S2), indicating that this relocalization is not a p53-mediated stress response but rather a result of the direct action of CX-3543.

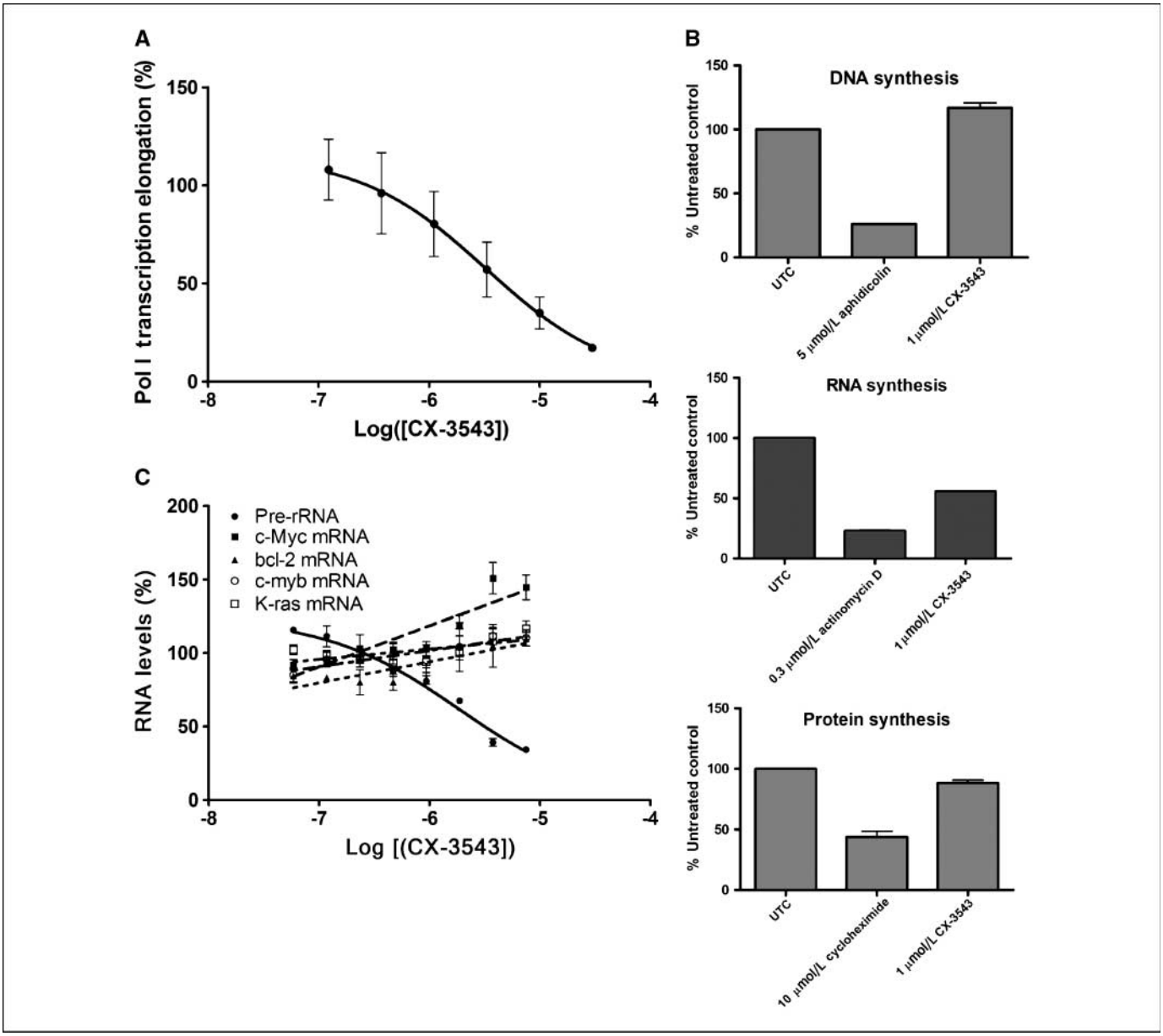

Figure 4. CX-3543 inhibits elongation by Pol I in isolated nuclei and selectively suppresses rRNA synthesis. *A,* effect of CX-3543 on nuclear run-on Pol I transcription. *B,* effects of CX-3543 on DNA, RNA, and protein synthesis. *C,* qRT-PCR analysis of the effects of CX-3543 on pre-rRNA, c-*myc*, bcl-2, c-myb, and k-ras mRNA levels in A549 cells.

Published OnlineFirst September 8, 2009; DOI: 10.1158/0008-5472.CAN-09-1304

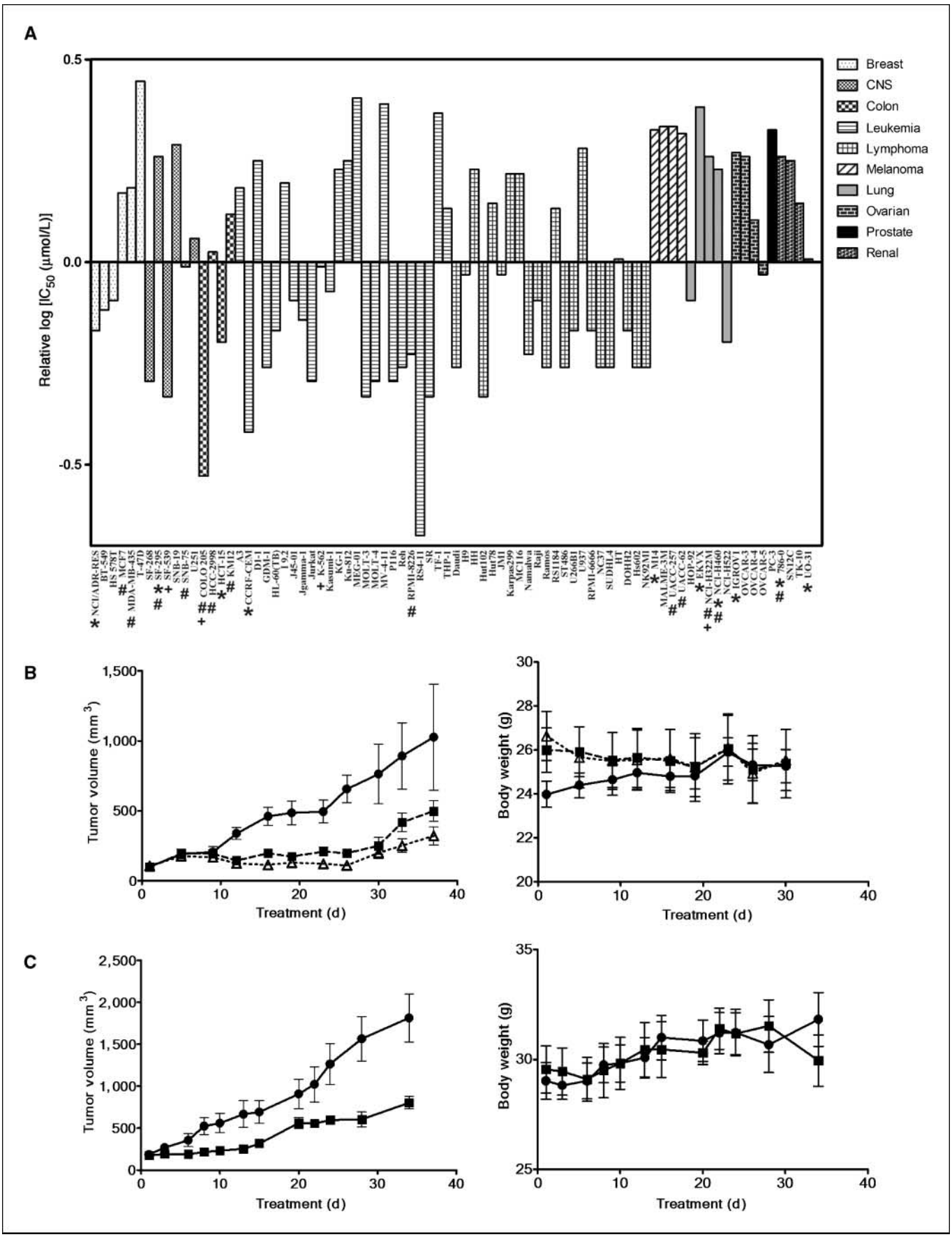

Published OnlineFirst September 8, 2009; DOI: 10.1158/0008-5472.CAN-09-1304

To test the selectivity of CX-3543 on disruption of nucleolin/rDNA G-quadruplex complexes relative to other nucleolar proteins/rDNA interactions, we used chromatin immunoprecipitation. Interrogation of three PQS-containing regions in the rDNA showed that treatment of A549 cells with CX-3543 caused nearly complete dissociation of nucleolin from all of them, whereas having little effect on the occupancy of nucleolin at the rDNA promoter or on the interaction of UBF or the TATA binding protein with the rDNA (Fig. 3*A*). The selectivity of CX-3543 toward nucleolin was supported by immunofluorescence analysis that showed CX-3543 can redistribute nucleolin without having any major effect on localization of another nucleolar protein, fibrillarin (Fig. 3*B*).

CX-3543 selectively inhibits rRNA synthesis by interfering with the elongation step of Pol I transcription. To test if CX-3543–mediated disruption of nucleolin/rDNA G-quadruplex complexes inhibits elongation of Pol I-driven transcription, we evaluated the effect of CX-3543 on the synthesis of rRNA by nuclear run-on assay. Isolated nuclei cannot initiate RNA synthesis *de novo*, and thus, all RNA synthesis that occurs in them is the result of the elongation of transcripts by RNA polymerases that already have initiated transcription (34). Inclusion of α-amanitin in the assay inhibits RNA Polymerases II and III (35) and thus allows the evaluation of the effects specific to elongation by Pol I. In the presence of α-amanitin, CX-3543 showed concentration-dependent inhibition of transcription in isolated nuclei with IC_{50} of 3.3 μmol/L (Fig. 4*A*).

The selectivity of CX-3543 toward the inhibition of RNA synthesis over DNA and protein synthesis was shown by studies measuring the incorporation of tritiated precursors in cells. In short, colorectal adenocarcinoma cells HCT 116 were treated for 2 hours with 1 μmol/L of CX-3543 or aphidicolin, actinomycin D, and cyclohexemide as controls, and the effects on [^{3}H]-uridine, [^{3}H]-thymidine, and [^{3}H]-methionine incorporation were measured. As can be seen from Fig. 4*B*, treatment with 1 μmol/L of CX-3543 resulted in ∼50% reduction in incorporation of [^{3}H]-uridine, whereas having no or little effect on [^{3}H]-thymidine and [^{3}H]-methionine uptake, indicating that CX-3543 preferentially inhibits RNA synthesis over DNA and protein synthesis. In contrast, another quadruplex-interacting compound BRACO-19, which is known to interfere with telomere function, was previously shown to preferentially inhibit DNA synthesis over RNA synthesis (36), supporting the notion that discrete G-quadruplex–binding pharmacophores may have alternative mechanisms of action.

In addition to *rRNA* genes, transcription of several oncogenes (including *bcl-2*, *c-myb*, c-*myc*, and *k-ras*) is thought to be controlled by formation of G-quadruplexes (37–40), and certain G-quadruplex–binding compounds were shown to modulate the transcription of these genes through stabilization of quadruplexes (38, 41). In contrast, although treatment of A549 cells with CX-3543 resulted in the dose-dependent suppression of rRNA synthesis with an IC_{50} of 1.8 μmol/L, it had no inhibitory effect on the RNA Polymerase II-driven transcription of *bcl-2*, *c-myb*, c-*myc*, and *k-ras* mRNAs (Fig. 4*C*).

CX-3543 does not cause cellular effects associated with telomere dysfunction. Although the majority of quadruplex-binding compounds are thought to exhibit their biological activity through the interference with telomerase function (reviewed in ref. 42), CX-3543 caused no cellular effects that are generally associated with telomeric dysfunction. Short-term (48 hours) treatment of A549 cells with a cytotoxic dose (1 μmol/L) of CX-3543 (IC_{50}, 0.4 μmol/L at 48 hours) did not cause telomeric fusions, polynucleated cells, or anaphase bridges, whereas prolonged exposure (16 days) of MCF7 breast carcinoma cell line that possess short telomeres (43), to subcytotoxic concentrations (200 nmol/L) of CX-3543 (IC_{50}, 1.3 μmol/L at 48 hours) had no effect on cell proliferation (Supplementary Fig. S3).

CX-3543 does not interfere with Topoisomerase I/II function in cells. Because certain fluoroquinolone-based agents were shown to interfere with Topoisomerase function (26), we evaluated the effect of CX-3543 on Topoisomerase activity. In a cell-free Topoisomerase II poisoning assay, as high as 100 μmol/L of CX-3543 had no effect on cleavable complex formation (data not shown), indicating that CX-3543 is not a Topoisomerase II poison. Both Topoisomerase I and II are known to participate in DNA replication (reviewed in ref. 44) and thus it is plausible to propose that drugs that interfere with Topoisomerase I/II function will have an effect on DNA synthesis. To test this, we evaluated the effects of CX-3543 or three controls, Irinotecan (Topoisomerase I poison), Mitoxantrone (Topoisomerase II poison), and Merbarone (Topoisomerase II catalytic inhibitor) on DNA synthesis and cell viability in A549 cells (see Supplementary Materials and Methods). The data presented in Supplementary Fig. S4 shows that all controls inhibited DNA synthesis at concentrations below those that had significant effects on cell viability. This means that poisoning of Topoisomerase I or Topoisomerase II, or even simple inhibition of Topoisomerase II catalytic activity results in the inhibition of DNA synthesis without immediate concomitant effects on cell viability. In contrast, the reduction in DNA synthesis by CX-3543 was only evident at concentrations where CX-3543 severely affected cell viability and hence was secondary to the antiproliferative effects of the drug. These data show that CX-3543 does not interfere with Topoisomerase I/II function in cells.

CX-3543 induces apoptosis in cancer cells. Inhibition of rRNA synthesis in cancer cell lines is known to cause nucleolar stress that results in disintegration of nucleoli and subsequent activation of the p53 response and apoptosis (45). Additionally, in a p53-null environment inhibition of rRNA synthesis can still produce an apoptotic response indicating the presence of compensatory pathways (46). As expected, the inhibition of rRNA synthesis by CX-3543 led to stabilization of p53 (data not shown) that was followed by induction of apoptosis, as judged by nuclear shrinkage, caspase-3 activation, cleavage of poly ADP ribose polymerase (PARP), and induction of chromatin DNA laddering (Supplementary Fig. S5). Interestingly, just like actinomycin D, CX-3543 was able to induce apoptotic response in p53-null cell line HL-60 (Supplementary Fig. S5*C*). In addition to stabilization of p53, treatment with actinomycin D was shown to induce phosphorylation of histone H2AX at Ser139 (γ-H2AX; ref. 47). The authors proposed that this event is mediated by kinase DNA-PK that in

Figure 5. CX-3543 shows anticancer activity *in vitro* and *in vivo*. *A,* effect of CX-3543 on cell viability of multiple cancer cell lines. The IC_{50} values were calculated with an average IC_{50} of 2.36 μmol/L. Relative logs of IC_{50} were plotted. Cell lines overexpressing multidrug resistance efflux pumps MDR1 (*), MXR (#), and MRP1 (+) are marked accordingly (56). *CNS,* central nervous system. *B,* MDA-MB-231 breast cancer xenograft model in which mice were treated once daily for a total of 37 d with vehicle (●), 6.25 mg/kg (■), or 12.5 mg/kg of CX-3543 (△) administered i.v. *C,* MIA PaCa-2 pancreatic cancer xenograft model in which mice were treated for a total of 13 d with vehicle (●) or 5 mg/kg of CX-3543 (■) administered i.v. once daily, followed by 7 d of rest, followed by 14 d of once daily treatment.

Published OnlineFirst September 8, 2009; DOI: 10.1158/0008-5472.CAN-09-1304

such case may serve as a sensor for stalled transcriptional bubbles. Alternatively, the γ-H2AX induction can be a result of DNA damage, because Actinomycin D was previously shown to induce DNA double-stranded breaks (48). Because the inhibition of Pol I elongation by CX-3543 should result in stalled transcription bubbles, we investigated the effects of CX-3543 on the phosphorylation status of H2AX. Whereas 4-hour treatment of A549 cells with 5 μmol/L of CX-3543 did not change the phosphorylation status of H2AX (data not shown), 8-hour treatment with the same dose resulted in a marked increase in phosphorylation of H2AX at Ser139 (Supplementary Fig. S6). Two-hour pretreatment of cells with a selective inhibitor of DNA-PK, AMA37, failed to prevent this phosphorylation, indicating that DNA-PK is not a major mediator of the CX-3543–triggered γ-H2AX induction. In addition to inhibition of transcription, cellular γ-H2AX levels can increase as a result of direct DNA damage, telomere injury, or apoptosis-driven DNA fragmentation (49, 50). CX-3543 tested negative in Ames and chromosome aberration genotoxicity assays and, as shown above, had no effect on Topoisomerase I/II function, indicating that the increase of γ-H2AX levels by CX-3543 does not result from the direct DNA damage. Several other quadruplex-binding compounds are known to induce DNA damage–like response through telomere injury (49, 51). Such telomere damage is usually associated with nuclear abnormalities (52, 53), which we did not observe in cells treated with CX-3543 (Supplementary Fig. S3), making this an unlikely explanation for the observed phenomenon. One other possibility is that γ-H2AX induction by CX-3543 results from apoptosis-driven DNA fragmentation (50). Induction of apoptosis was evident in A549 cells treated for 8 hours with 5 μmol/L of CX-3543, as judged by PARP cleavage. Two-hour preincubation of cells with 50 μmol/L of pan-caspase inhibitor Z-VAD(OMe)-FMK was able to suppress caspase activation, blocking the cleavage of PARP and also inhibiting the induction of γ-H2AX by CX-3543 (Supplementary Fig. S6). This result indicates that phosphorylation of H2AX in cells treated with CX-3543 is most likely due to double-stranded DNA breaks introduced by caspase-activated DNase, and thus is secondary to the induction of the apoptosis by the drug.

CX-3543 exhibits broad antiproliferative activity *in vitro*. When evaluated against 80 cell lines representing an expansion of the National Cancer Institute (NCI) 60 cell panel, CX-3543 was found to exert a broad range of *in vitro* antiproliferative activity (see Supplementary Materials and Methods; Fig. 5*A*). COMPARE analysis of these data[3] indicates a unique mode of action for CX-3543, as the range of action profile, does not correlate with any compound in the current NCI database. Moreover, cancer cell lines overexpressing MDR1, MXR, or MRP1 drug resistance transporter genes retained sensitivity to CX-3543, indicating CX-3543 is not a substrate for these multidrug resistance pumps (Fig. 5*A*).

CX-3543 exhibits antitumor activity *in vivo*. A broad range of antitumor activity was observed *in vivo* in murine xenograft models of multiple human cancers, including breast (MDA-MB-231), wherein daily treatment with CX-3543 (6.25 or 12.5 mg/kg) was well-tolerated and suppressed tumor growth (Fig. 5*B*). Similarly, treatment of mice bearing MIA PaCa-2 pancreatic xenografts with CX-3543 (5 mg/kg) for 13 days resulted in significant inhibition of tumor growth with minimal effect on animal body weights (Fig. 5*C*). CX-3543 dosing was halted during days 14 to 20 to allow a drug holiday. Upon resumption of dosing during days 21 to 26, tumor growth was again inhibited, indicating that tumors retained sensitivity and had not developed resistance to CX-3543 during the course of treatment or holiday.

Discussion

As the role of excessive rRNA synthesis in tumorigenesis comes to be better understood (reviewed in refs. 6, 7, 54), the therapeutic potential of drugs to target this process becomes more evident. The recent discovery that loss of certain tumor-suppressors, an aberration commonly found in cancer, makes cells more susceptible to death in response to rRNA synthesis inhibition, suggests that a good therapeutic window can be achieved with anticancer drugs that specifically target Pol I transcription (54). Herein, we report an innovative anticancer therapeutic approach that is based on the direct suppression of the rRNA biogenesis by a small molecule agent, CX-3543 that displaces nucleolin from PQSs on the nontemplate strand of rDNA, causing rapid redistribution of nucleolin from nucleoli, inhibition of rRNA synthesis, and apoptotic death in cancer cells.

Our data indicate that CX-3543 is quite selective in its mechanism of action. It is able to suppress rRNA synthesis while having no inhibitory effects on DNA and protein synthesis, RNA polymerase II–driven transcription of oncogenes, or Topoisomerase I/II function. Furthermore, CX-3543 failed to elicit biological responses indicative of interference with telomere function. The selectivity achieved toward targeting Pol I transcription is potentially explained by the cellular distribution and pharmacokinetic properties of CX-3543. We have shown that CX-3543 concentrates in nucleoli (Fig. 1*B*) where rRNA is synthesized and has not been observed in the nucleoplasm, where the majority of telomeres are present and where RNA Polymerases II–driven transcription of oncogenes occurs.

CX-3543 exhibited broad *in vitro* antiproliferative and *in vivo* antitumor activity and was well tolerated in murine xenograft studies at efficacious doses (Fig. 5). Numerous attempts to isolate cancer cells (MIA PaCa-2 pancreatic and HCT-116 colorectal cancer cells) resistant to CX-3543 were unsuccessful using three separate techniques (selection of naturally occurring resistant mutants, induction of resistant mutants by UV-mediated mutagenesis, and dominant suppressor analysis using a human cDNA expression library; data not shown). Preliminary assessments suggest CX-3543 is not a substrate for multidrug resistance pumps and *in vivo* responses are durable. These data suggest a low tendency to acquire and develop resistance to CX-3543 and could prove to be a key differentiating factor relative to other anticancer drugs in the clinical setting.

CX-3543 has recently completed two separate phase I clinical trials using different dosing schedules in patients with solid tumors. During the phase I trial, the maximum concentration (C_{max}) values attained in human whole blood when CX-3543 was infused over 6 hours at 360 mg/m^2 on the daily ×5 schedule reached 3 to 5 μmol/L. The blood levels achieved clinically are well within the range of *in vitro* potency observed for CX-3543. In addition, CX-3543 was well tolerated, showed a long plasma half-life, and displayed evidence of biological activity in patients with carcinoid/neuroendocrine tumors (55). Moreover, preclinical biodistribution studies in rodents revealed that CX-3543 accumulates in tissues derived from the neural crest, i.e., those tissues

[3] http://dtp.nci.nih.gov/docs/compare/compare_methodology.html

Published OnlineFirst September 8, 2009; DOI: 10.1158/0008-5472.CAN-09-1304

that give rise to carcinoid/neuroendocrine tumors. As a result of these scientific and clinical findings, CX-3543 was advanced into phase II clinical trial in patients having carcinoid/neuroendocrine tumors.

Our findings support a basis for direct targeting of rRNA biogenesis as a strategy for selective induction of apoptosis in cancer cells and pave the way for an entirely new class of anticancer therapeutics.

Disclosure of Potential Conflicts of Interest

D. Drygin, A. Siddiqui-Jain, S. O'Brien, M. Schwaebe, A. Lin, J. Bliesath, C.B. Ho, C. Proffitt, K. Trent, J.P. Whitten, J.K.C. Lim, K. Anderes, and W.G. Rice are employees of Cylene Pharmaceuticals. D. Von Hoff is a consultant and an advisory board member for Cylene Pharmaceuticals.

Acknowledgments

Received 4/8/09; revised 6/30/09; accepted 7/22/09; published OnlineFirst 9/8/09.

Grant support: Supported by Cylene Pharmaceuticals. All authors are affiliated with Cylene Pharmaceuticals.

The costs of publication of this article were defrayed in part by the payment of page charges. This article must therefore be hereby marked *advertisement* in accordance with 18 U.S.C. Section 1734 solely to indicate this fact.

We thank Ms. Nicole Streiner for her significant contribution to identification of CX-3543, Dr. David Ryckman for his contribution to the manufacturing and formulation of CX-3543, Drs. Jerry Birnbaum and Nancy Maizels for critically reviewing the manuscript, and Dr. Walter Gilbert for stimulating discussions.

References

1. Ruggero D, Pandolfi PP. Does the ribosome translate cancer? Nat Rev Cancer 2003;3:179–92.
2. Moss T, Langlois F, Gagnon-Kugler T, Stefanovsky V. A housekeeper with power of attorney: the rRNA genes in ribosome biogenesis. Cell Mol Life Sci 2007;64:29–49.
3. Chedin S, Laferte A, Hoang T, Lafontaine DL, Riva M, Carles C. Is ribosome synthesis controlled by pol I transcription? Cell Cycle 2007;6:11–5.
4. Grummt I. Regulation of mammalian ribosomal gene transcription by RNA polymerase I. Prog Nucleic Acid Res Mol Biol 1999;62:109–54.
5. White RJ. RNA polymerases I and III, growth control and cancer. Nat Rev Mol Cell Biol 2005;6:69–78.
6. Montanaro L, Trere D, Derenzini M. Nucleolus, ribosomes, and cancer. Am J Pathol 2008;173:301–10.
7. White RJ. RNA polymerases I and III, non-coding RNAs and cancer. Trends Genet 2008;24:622–9.
8. Maggi LB, Jr., Weber JD. Nucleolar adaptation in human cancer. Cancer Invest 2005;23:599–608.
9. Arabi A, Wu S, Ridderstrale K, et al. c-Myc associates with ribosomal DNA and activates RNA polymerase I transcription. Nat Cell Biol 2005;7:303–10.
10. Zhai W, Comai L. Repression of RNA polymerase I transcription by the tumor suppressor p53. Mol Cell Biol 2000;20:5930–8.
11. Hannan KM, Hannan RD, Smith SD, Jefferson LS, Lun M, Rothblum LI. Rb and p130 regulate RNA polymerase I transcription: Rb disrupts the interaction between UBF and SL-1. Oncogene 2000;19:4988–99.
12. Zhang C, Comai L, Johnson DL. PTEN represses RNA Polymerase I transcription by disrupting the SL1 complex. Mol Cell Biol 2005;25:6899–911.
13. Pianese G. Beitrag zur Histologie und Aetiologie der Carcinoma Histologische und experimentelle Untersuchungen. Beitr Pathol Anat Allgem Pathol 1896;142:1–193.
14. Derenzini M, Trere D, Pession A, Govoni M, Sirri V, Chieco P. Nucleolar size indicates the rapidity of cell proliferation in cancer tissues. J Pathol 2000;191:181–6.
15. Williamson D, Lu YJ, Fang C, Pritchard-Jones K, Shipley J. Nascent pre-rRNA overexpression correlates with an adverse prognosis in alveolar rhabdomyosarcoma. Genes Chromosomes Cancer 2006;45:839–45.
16. Jordan P, Carmo-Fonseca M. Cisplatin inhibits synthesis of rRNA *in vivo*. Nucleic Acids Res 1998;26:2831–6.
17. Ghoshal K, Jacob ST. An alternative molecular mechanism of action of 5-fluorouracil, a potent anticancer drug. Biochem Pharmacol 1997;53:1569–75.
18. Fraschini A, Bottone MG, Scovassi AI, et al. Changes in extranucleolar transcription during actinomycin D-induced apoptosis. Histol Histopathol 2005;20:107–17.
19. Duquette ML, Handa P, Vincent JA, Taylor AF, Maizels N. Intracellular transcription of G-rich DNAs induces formation of G-loops, novel structures containing G4 DNA. Genes Dev 2004;18:1618–29.
20. French SL, Osheim YN, Cioci F, Nomura M, Beyer AL. In exponentially growing Saccharomyces cerevisiae cells, rRNA synthesis is determined by the summed RNA polymerase I loading rate rather than by the number of active genes. Mol Cell Biol 2003;23:1558–68.
21. Hershman SG, Chen Q, Lee JY, et al. Genomic distribution and functional analyses of potential G-quadruplex-forming sequences in Saccharomyces cerevisiae. Nucleic Acids Res 2008;36:144–56.
22. Srivastava M, Pollard HB. Molecular dissection of nucleolin's role in growth and cell proliferation: new insights. FASEB J 1999;13:1911–22.
23. Rickards B, Flint SJ, Cole MD, LeRoy G. Nucleolin is required for RNA polymerase I transcription *in vivo*. Mol Cell Biol 2007;27:937–48.
24. Storck S, Thiry M, Bouvet P. Conditional knockout of nucleolin in DT40 cells reveals the functional redundancy of its RNA-binding domains. Biol Cell 2009;101:153–67.
25. Hanakahi LA, Sun H, Maizels N. High affinity interactions of nucleolin with G-G-paired rDNA. J Biol Chem 1999;274:15908–12.
26. Wolfson JS, Hooper DC. Fluoroquinolone antimicrobial agents. Clin Microbiol Rev 1989;2:378–424.
27. Lin CY, Navarro S, Reddy S, Comai L. CK2-mediated stimulation of Pol I transcription by stabilization of UBF-SL1 interaction. Nucleic Acids Res 2006;34:4752–66.
28. Huppert JL, Balasubramanian S. Prevalence of quadruplexes in the human genome. Nucleic Acids Res 2005;33:2908–16.
29. Eddy J, Maizels N. Gene function correlates with potential for G4 DNA formation in the human genome. Nucleic Acids Res 2006;34:3887–96.
30. Todd AK, Johnston M, Neidle S. Highly prevalent putative quadruplex sequence motifs in human DNA. Nucleic Acids Res 2005;33:2901–7.
31. Ghisolfi-Nieto L, Joseph G, Puvion-Dutilleul F, Amalric F, Bouvet P. Nucleolin is a sequence-specific RNA-binding protein: characterization of targets on pre-ribosomal RNA. J Mol Biol 1996;260:34–53.
32. Daniely Y, Borowiec JA. Formation of a complex between nucleolin and replication protein A after cell stress prevents initiation of DNA replication. J Cell Biol 2000;149:799–810.
33. Daniely Y, Dimitrova DD, Borowiec JA. Stress-dependent nucleolin mobilization mediated by p53-nucleolin complex formation. Mol Cell Biol 2002;22:6014–22.
34. Hirayoshi K, Lis JT. Nuclear run-on assays: assessing transcription by measuring density of engaged RNA polymerases. Methods Enzymol 1999;304:351–62.
35. Kersten H, Kersten W. Inhibitors of nucleic acid synthesis: biophysical and biochemical aspects. Mol Biol Biochem Biophys 1974;18:1–184.
36. Gunaratnam M, Greciano O, Martins C, et al. Mechanism of acridine-based telomerase inhibition and telomere shortening. Biochem Pharmacol 2007;74:679–89.
37. Dexheimer TS, Sun D, Hurley LH. Deconvoluting the structural and drug-recognition complexity of the G-quadruplex-forming region upstream of the bcl-2 P1 promoter. J Am Chem Soc 2006;128:5404–15.
38. Hurley LH, Von Hoff DD, Siddiqui-Jain A, Yang D. Drug targeting of the c-MYC promoter to repress gene expression via a G-quadruplex silencer element. Semin Oncol 2006;33:498–512.
39. Palumbo SL, Memmott RM, Uribe DJ, Krotova-Khan Y, Hurley LH, Ebbinghaus SW. A novel G-quadruplex-forming GGA repeat region in the c-myb promoter is a critical regulator of promoter activity. Nucleic Acids Res 2008;36:1755–69.
40. Cogoi S, Xodo LE. G-quadruplex formation within the promoter of the KRAS proto-oncogene and its effect on transcription. Nucleic Acids Res 2006;34:2536–49.
41. Ou TM, Lu YJ, Zhang C, et al. Stabilization of G-quadruplex DNA and down-regulation of oncogene c-myc by quindoline derivatives. J Med Chem 2007;50:1465–74.
42. De Cian A, Lacroix L, Douarre C, et al. Targeting telomeres and telomerase. Biochimie 2008;90:131–55.
43. Raymond E, Sun D, Izbicka E, et al. A human breast cancer model for the study of telomerase inhibitors based on a new biotinylated-primer extension assay. Br J Cancer 1999;80:1332–41.
44. Champoux JJ. DNA topoisomerases: structure, function, and mechanism. Annu Rev Biochem 2001;70:369–413.
45. Huang M, Ji Y, Itahana K, Zhang Y, Mitchell B. Guanine nucleotide depletion inhibits pre-ribosomal RNA synthesis and causes nucleolar disruption. Leuk Res 2008;32:131–41.
46. Martin SJ, Lennon SV, Bonham AM, Cotter TG. Induction of apoptosis (programmed cell death) in human leukemic HL-60 cells by inhibition of RNA or protein synthesis. J Immunol 1990;145:1859–67.
47. Mischo HE, Hemmerich P, Grosse F, Zhang S. Actinomycin D induces histone γ-H2AX foci and complex formation of γ-H2AX with Ku70 and nuclear DNA helicase II. J Biol Chem 2005;280:9586–94.
48. Ross WE, Bradley MO. DNA double-stranded breaks in mammalian cells after exposure to intercalating agents. Biochim Biophys Acta 1981;654:129–34.
49. Salvati E, Leonetti C, Rizzo A, et al. Telomere damage induced by the G-quadruplex ligand RHPS4 has an antitumor effect. J Clin Invest 2007;117:3236–47.
50. Rogakou EP, Nieves-Neira W, Boon C, Pommier Y, Bonner WM. Initiation of DNA fragmentation during apoptosis induces phosphorylation of H2AX histone at serine 139. J Biol Chem 2000;275:9390–5.
51. Tauchi T, Shin-Ya K, Sashida G, et al. Activity of a novel G-quadruplex-interactive telomerase inhibitor, telomestatin (SOT-095), against human leukemia cells: involvement of ATM-dependent DNA damage response pathways. Oncogene 2003;22:5338–47.
52. Leonetti C, Amodei S, D'Angelo C, et al. Biological activity of the G-quadruplex ligand RHPS4 (3,11-difluoro-6,8,13-trimethyl-8H-quino[4,3,2-kl]acridinium methosulfate) is associated with telomere capping alteration. Mol Pharmacol 2004;66:1138–46.
53. Phatak P, Cookson JC, Dai F, et al. Telomere uncapping by the G-quadruplex ligand RHPS4 inhibits clonogenic tumour cell growth *in vitro* and *in vivo* consistent with a cancer stem cell targeting mechanism. Br J Cancer 2007;96:1223–33.
54. Montanaro L, Mazzini G, Barbieri S, et al. Different effects of ribosome biogenesis inhibition on cell proliferation in retinoblastoma protein- and p53-deficient and proficient human osteosarcoma cell lines. Cell Prolif 2007;40:532–49.
55. Lim JK, Padgett CS, Von Hoff DD, et al. Quarfloxin phase I clinical data and scientific findings supporting the selection of carcinoid/neuroendocrine tumors as the phase II indication. In: 100th AACR Annual Meeting 2009 Proceedings; 2009 April 18–22; Denver, CO, U S A. p. 868–69.
56. Szakács G, Annereau JP, Lababidi S, et al. Predicting drug sensitivity and resistance: profiling ABC transporter genes in cancer cells. Cancer Cell 2004;6:129–37.

Cancer Research
The Journal of Cancer Research (1916–1930) | The American Journal of Cancer (1931–1940)

AACR American Association for Cancer Research

Anticancer Activity of CX-3543: A Direct Inhibitor of rRNA Biogenesis

Denis Drygin, Adam Siddiqui-Jain, Sean O'Brien, et al.

Cancer Res 2009;69:7653-7661. Published OnlineFirst September 8, 2009.